Simulation and Experiments on the Capillary Force between a Circular Disk and a Parallel Substrate *

Le-Feng Wang(王乐锋), Ben-Song Huang(黄本松), Yuan-Zhe He(何元哲),
Wei-Bin Rong(荣伟彬)**, Li-Ning Sun(孙立宁)

State Key Laboratory of Robotics and System, Harbin Institute of Technology, Harbin 150080

(Received 3 January 2017)

The capillary force of a liquid bridge with a pinned contact line between a small disk and a parallel plate is investigated by simulation and experiments. The numerical minimization simulation method is utilized to calculate the capillary force. The results show excellent agreement with the Young–Laplace equation method. An experimental setup is built to measure the capillary force. The experimental results indicate that the simulation results agree well with the measured forces at large separation distances, while some deviation may occur due to the transition from the advancing contact angle to the receding one at small distances. It is also found that the measured rupture distance is slightly larger than the simulation value due to the effect of the viscous interaction inside the liquid bridge.

PACS: 68.03.Cd, 68.08.−p, 47.55.dr DOI: 10.1088/0256-307X/34/5/056801

The research on capillary forces between two solids with mediated liquid has a long history for their practical applications in a wide range of scientific and industrial fields.[1−3] In recent years, it gained a great deal of attention due to its relation to force measurement of atomic force microscopy,[4] self-assembly,[5] microobjects manipulation,[6] nanofluidics,[7] liquid bearing,[8,9] biologic attachment mechanism,[10,11] and so on.

As typical configurations, capillary forces between two spheres, between a sphere and a plate have been widely studied.[12−16] For another configuration, the capillary force between two parallel plates has also been investigated theoretically. Carter calculated the force between two parallel plates with the mediated liquid bridge.[17] The liquid has the same contact angles on the two plates. Forters investigated the liquid bridge between two parallel plates.[18] The r bridge that the fluid interface touches the plate circumference and the θ bridge that the fluid interface does not touch the plate circumference were distinguished from each other. The liquid bridge is also symmetric about the midplane. The liquid bridge force between two chemically different substrates for the θ bridge was also studied.[19]

For a liquid bearing or a biological attachment device, the liquid bridge that connects a finite upper disk and a substrate can be analyzed as a simplified model. Qian *et al.*[20] investigated the scaling effects of the capillary force between a fiber and a solid surface based on the Young–Laplace equation. It was pointed out that the adhesive strength can be enhanced by contact size reduction. Qian *et al.*[21] studied the shape of a stretching liquid bridge between a disk and a substrate on the basis of the Young–Laplace equation. Due to the fact that the double iterative method was adopted based on the classical equation, tedious computation was needed. Moreover, direct experimental comparison with theoretical results was not shown for the capillary force of the liquid bridge with a pinned contact line between a disk and a substrate.

In this Letter, we investigate the capillary force of the liquid bridge with a pinned contact line between a circular disk and a parallel substrate by simulation and experiments. A numerical minimization of the interfacial energy method is adopted to obtain the capillary force between the disk and the substrate. The obtained capillary force is compared with available results based on the Young–Laplace equation. The experimental results will also be compared with the simulation ones.

Figure 1 shows the schematic diagram of an axisymmetric liquid bridge with a pinning contact line between a circular disk and a parallel substrate. The upper disk is a cylindrical disk with a radius of R. Here $\theta_{\rm A}$ is the pinning contact angle of the liquid on the upper disk, $\theta_{\rm B}$ is the contact angle of the liquid on the lower plate, and D is the separation distance between the disk and the plate.

To perform the minimization of the system free energy, the Surface Evolver software is utilized to model the liquid bridge with a pinned contact line. Surface Evolver is a finite element solver utilizing the gradient descent method to minimize the total free energy of a surface subject to given boundary constraints. The total energy contains the interfacial energy and the gravitational energy. Since the effect of gravity is negligible compared with the surface tension for liquid of small volume in our study, the total free energy can be described as

$$E = \gamma_{\rm LV} A_{\rm LV} + (\gamma_{\rm LS} - \gamma_{\rm VS}) A_{\rm LS}, \quad (1)$$

*Supported by the Foundation for Innovative Research Groups of the National Natural Science Foundation of China under Grant No 51521003, and the Self-Planned Task of State Key Laboratory of Robotics and System under Grant No SKLRS201501A04.

**Corresponding author. Email: weibinrong@126.com

© 2017 Chinese Physical Society and IOP Publishing Ltd

where $\gamma_{\rm LV}$ refers to the surface tension of the liquid droplet, $\gamma_{\rm LS}$ and $\gamma_{\rm VS}$ refer to the interfacial tensions of the liquid-solid and vapor-solid interfaces, respectively, $A_{\rm LV}$ and $A_{\rm LS}$ denote the areas of the liquid-vapor and liquid-solid interfaces, respectively. With the help of Surface Evolver, the equilibrium formation of the liquid bridge could be forecasted accurately. The capillary force can be calculated from the first derivative of the total energy with respect to the distance. Additionally, the rupture distance of the liquid bridge can be obtained by searching for the maximum distance of the liquid bridge at an equilibrium state under the specified constraint conditions.

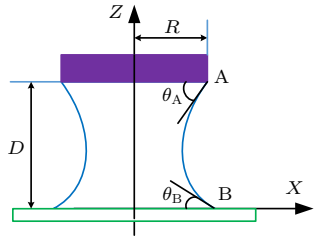

Fig. 1. The liquid bridge between a circular disk and a parallel plate.

To verify the simulation results based on the minimization of the system free energy, the method based on the Young–Laplace equation will also be demonstrated here. According to the Young–Laplace equation, the equilibrium profile of the liquid bridge can be illustrated by the following ordinary differential equation

$$-\frac{X''}{(1+X'^2)^{3/2}}+\frac{1}{X(1+X'^2)^{1/2}}=\frac{\Delta P}{\gamma}, \quad (2)$$

where ΔP is the pressure difference between the inside and outside of the liquid, and γ is the surface tension of the liquid. With the following normalization by the upper disk radius R, the equation system can be rewritten as

$$-\frac{x''}{(1+x'^2)^{3/2}}+\frac{1}{x(1+x'^2)^{1/2}}=\frac{R\Delta P}{\gamma}=\Delta p, \quad (3)$$

where $x=X/R$, and $z=Z/R$.

The liquid volume V is nondimensionalized by R^3

$$v=V/R^3=\int_{z_{\rm B}}^{z_{\rm A}}\pi x^2 dz. \quad (4)$$

The initial condition of the liquid profile at point B is

$$\frac{dx}{dz}\Big|_{z=0}=\begin{cases}-\frac{1}{\tan\theta_{\rm B}}, & \theta_{\rm B}\neq\frac{\pi}{2},\\ 0, & \theta_{\rm B}=\frac{\pi}{2}.\end{cases} \quad (5)$$

For a given dimensionless liquid volume v, a circular disk radius R and a separation distance D, the contact angle on the upper disk $\theta_{\rm A}$ is assumed firstly, then Eq. (2) can be solved by a numerical iteration method to obtain the specific liquid bridge profile.[19]

Once the profile of the liquid bridge is obtained, the capillary force exerting on the upper disk can be calculated. The dimensionless capillary force $f=F/(\gamma R)$ is then

$$f=2\pi x_{\rm A}\sin\theta_{\rm A}-\Delta p\pi x_{\rm A}^2. \quad (6)$$

To theoretically analyze the effects of related parameters on the capillary force between a circular disk and a parallel substrate, a group of contact angles on the substrate $\theta_{\rm B}$ are selected as 30°, 60°, 90°, 120° and 150°. Figure 2 shows the relationship between the dimensionless force and the dimensionless distance at different contact angles using the energy minimization method and the Young–Laplace equation method, respectively. We can see that the energy minimization method shows excellent agreement with the Young–Laplace equation method. This indicates that both the methods are reliable to compute the capillary force between a small disk and a substrate with a pinned contact line.

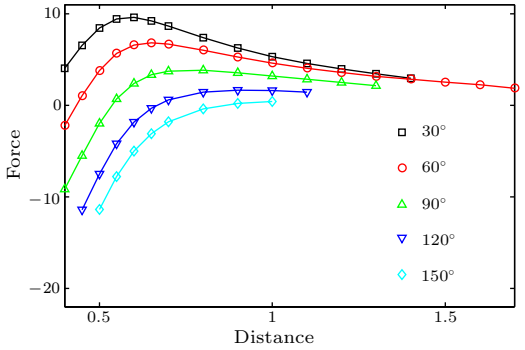

Fig. 2. The relationship of the dimensionless force and the dimensionless distance at $v=2$. The solid line denotes the result from the energy method, and the symbol dots denote the result from the Young–Laplace equation method.

From Fig. 2, it can be seen that the dimensionless attractive force increases with the dimensionless distance for small contact angles firstly, after a maximum value is achieved, the force decreases with the distance. This is very different from the θ bridge between two infinite parallel plates. For the θ bridge, the capillary force decreases gradually with the increasing distance for two hydrophilic surfaces.[18] With the increase of the contact angle, the attractive force decreases gradually for a given dimensionless distance. The interaction force may become being repulsive in the whole separation process when the contact angle is very large.

To measure the capillary force exerting on the upper disk, an experimental setup was built on the base of the schematic diagram shown in Fig. 3. Dipropylene glycol butyl ether (surface tension $\gamma=28.4\,{\rm mN/m}$, density $\rho=0.91\,{\rm g/cm^3}$) and ethylene glycol (surface tension $\gamma=46.5\,{\rm mN/m}$, density $\rho=1.11\,{\rm g/cm^3}$) are utilized to form the liquid bridge. We use glass slides treated by 1,1,2,2-tetrahydroperfluorodecyltrimethoxysilane as the lower plates, whose receding contact angles for dipropylene glycol butyl ether and ethylene glycol are 39° and 68°,

respectively. The upper disk is a cylindrical brass disk with a radius of 0.5 mm, which is attached to the moving part of a Z-axis motion platform. The Z-axis platform is utilized to control the position of the upper disk. A precision electric balance (BT25S, Sartorius AG, Germany) with the resolution of 10 μg was adopted to measure the capillary forces exerted on the upper disk. A camera (acA645-100gm, Basler AG, Germany) equipped with a magnifying lens is utilized to capture the tracks of the upper disk and the evolution of the liquid bridge shape.

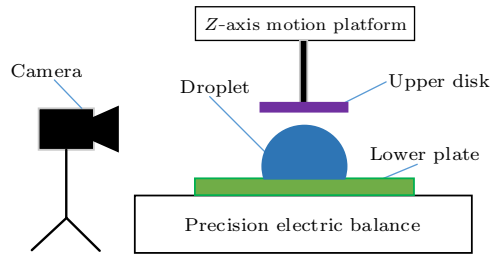

Fig. 3. The schematic diagram of the experimental setup.

The liquid bridge between the upper disk and the lower plate was developed in the following. A pipet was used to deposit a droplet of liquid on the lower plate. The volume of the droplet in our experiments was calculated by analyzing the droplet images acquired from the camera. Initially, the cylindrical disk was positioned above the liquid droplet. Then it was moved downwards and a liquid bridge forms between the disk and the lower plate. When the specified position was reached, the disk was moved upwards until the liquid bridge ruptured. The velocity of the moving cylindrical disk was maintained at 10 μm/s. The recording frequency of forces by the electric balance is 5 Hz. In all our experiments, the ambient temperature was controlled at 25℃, and the humidity is about 38.5%.

The experimental force-distance curves of capillary forces for the two liquids are shown in Fig. 4. For the liquid bridges in Figs. 4(a) and 4(b), the liquid volumes are 0.1552 μL and 0.2763 μL, respectively. The Bond number can be defined as $Bo = \rho g l^2/\gamma$, where g is the gravitational acceleration, and l is the characteristic length of the liquid bridge. The Bond numbers are both much less than 1, and this indicates that the surface tension dominates the gravitational force. The simulation results from Surface Evolver are also plotted for contrast. For the simulation curve, the receding contact angles of 39° and 68° were adopted for dipropylene glycol butyl ether and ethylene glycol, respectively. It can be seen that the experimental values of capillary forces agree well with the simulation results when the separation distance is large. The experimental curves also display a maximum attractive force, but the position of the maximum value changes in comparison to the simulation curve. Additionally, when the distance is small, the measured force curves are below the simulation one. This can be attributed to the contact angle hysteresis. When the separation is small, the contact angle on the lower plate decreases from an advancing angle to the receding angle during the stretching, thus larger contact angles lead to smaller attractive forces. As the distance is increased further, the contact angle reaches the receding value and remains almost constant, thus the capillary force is consistent with the simulation value subsequently. Figures 5(a) and 5(b) show the images of advancing and receding liquid bridge for ethylene glycol, respectively. From the images, the measured advancing and receding contact angles are 85° and 68°, respectively.

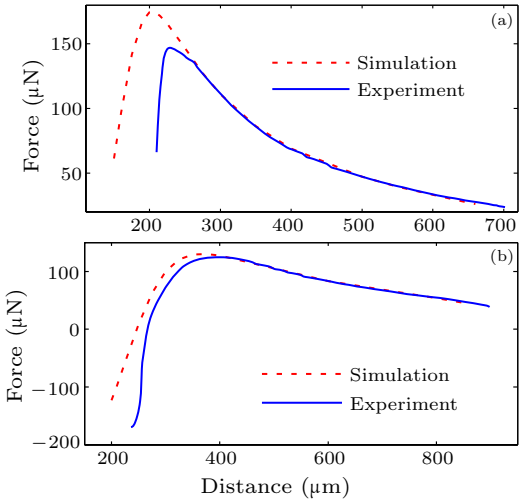

Fig. 4. Comparison of simulation and experimental force-distance curves for different liquids: (a) dipropylene glycol butyl ether and (b) ethylene glycol.

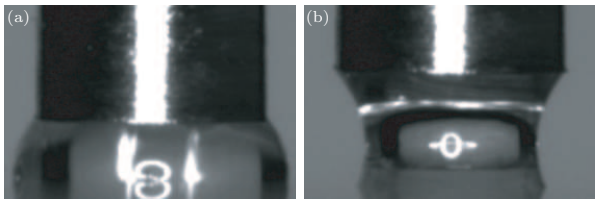

Fig. 5. Images of liquid menisci of ethylene glycol when the upper disk (a) approaches or (b) retracts the lower plate.

The rupture distances of the liquid bridge were obtained by analyzing images of the liquid bridge. The simulation study was carried out using Surface Evolver by searching for the maximum distance of liquid bridge at equilibrium state under the specified constraint conditions. Compared with the simulation result, the actual rupture distance increases about 4.5% averagely. The increase can be partly attributed to the viscous forces inside the liquid bridge that can be helpful to stabilize the stretching bridge.[22] Moreover, the molecular friction at microscale affects the energy dissipation in the dynamic evolution process of the liquid bridge.[23]

To compare the compressing and stretching process of the liquid bridge, a back-and-forth movement of the upper disk was implemented, and the forces

during the process were recorded continually. The typical force-distance curve for the ethylene glycol liquid bridge is given in Fig. 6. It shows that the force during stretching is smaller than that during compressing for the same separation distance. This is also attributed to the transition of the contact angles on the substrate from the advancing contact angle to the receding one during the process.

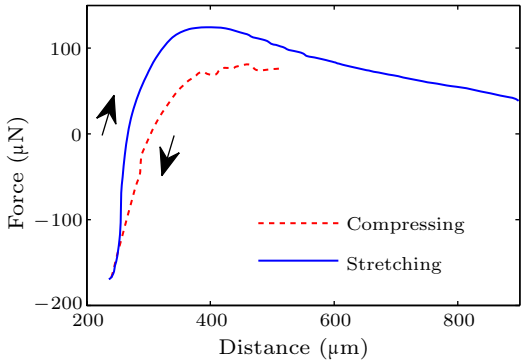

Fig. 6. The force-distance curve of ethylene glycol droplet during a back-and-forth process.

In summary, we have investigated the capillary force of the liquid bridge with a pinned contact line between a small disk and a parallel plate by simulation and experiments. The numerical minimization method shows an excellent agreement with the method based on the Young–Laplace equation. The force-distance curves show maximum values of forces with the increased distance for hydrophilic substrates. The rupture distance of the liquid bridge is slightly larger than the simulation result partly due to the effect of viscous force inside the liquid bridge. Moreover, the hysteresis of the contact angle may lead to different capillary forces during the compressing and stretching processes. These results are helpful in designing a liquid bearing system and understanding the biological attachment mechanism.

References

[1] Young T 1805 *Philos. Trans. R. Soc.* **95** 65
[2] Fisher R 1926 *J. Agric. Sci.* **16** 492
[3] Butt H J and Kappl M 2009 *Adv. Colloid Interface Sci.* **146** 48
[4] Tabor R F, Grieser F, Dagastine R R and Chan D Y 2012 *J. Colloid Interface Sci.* **371** 1
[5] Dasgupta S, Katava M, Faraj M, Auth T and Gompper G 2014 *Langmuir* **30** 11873
[6] Fan Z H, Wang L F, Rong W B and Sun L N 2015 *Appl. Phys. Lett.* **106** 084105
[7] Chen J G, Wang C L, Wei N, Wan R Z and Gao Y 2016 *Nanoscale* **8** 5676
[8] Yoxall B E, Chan M L, Harake R S, Pan T and Horsley D A 2012 *J. Microelectromech. S.* **21** 721
[9] Takei A, Matsumoto K and Shomoyama I 2010 *Lab Chip* **10** 1781
[10] Labonte D and Federle W 2014 *Philos. Trans. R. Soc.B* **370** 20140027
[11] Autumn K, Niewiarowski and Puthoff J B 2014 *Annu. Rev. Ecol. Evol. Syst.* **45** 445
[12] Willett C D, Adams M J, Johnson S A and Seville J P K 2000 *Langmuir* **16** 9396
[13] Wang L F, Rong W B, Sun L N, Chen L G and Shao B 2009 *Chin. Phys. Lett.* **26** 126801
[14] Zheng W and Zhao Y P 2004 *Chin. Phys. Lett.* **21** 616
[15] Lambert P and Delchambre A 2005 *Langmuir* **21** 9537
[16] Rabinovich Y I, Esayanur M S and Moudgil B M 2005 *Langmuir* **21** 10992
[17] Carter W C 1988 *Acta Metall.* **36** 2283
[18] Fortes M A 1982 *J. Colloid Interface Sci.* **88** 338
[19] De Souza E J, Brinkmann M, Mohrdieck C, Crosby A and Arzt E 2008 *Langmuir* **24** 10161
[20] Qian J and Gao H 2006 *Acta Biomater.* **2** 51
[21] Qian B and Breuer K S 2011 *J. Fluid Mech.* **666** 554
[22] Zhang X, Padgett R S and Basaran O A 1996 *J. Fluid Mech.* **329** 207
[23] Yuan Q Z, Huang X F and Zhao Y P 2014 *Phys. Fluids* **26** 092104